CRACK MICROSTRUCTURE DURING THE CARBONIZATION OF CARBON FIBRE REINFORCED PLASTICS TO CARBON/CARBON COMPOSITES

J. Schulte-Fischedick [1], M.Frieß [1], W.Krenkel [1], R.Kochendörfer[1] and M.König [2]

[1]*Institute of Structures and Design, German Aerospace Center (DLR), Pfaffenwaldring 38/40, 70569 Stuttgart*
[2] *Institute of Statics and Dynamics in Aerospace Structures, University of Stuttgart, Pfaffenwaldring 27, D- 70550 Stuttgart*

SUMMARY: The major process for manufacturing carbon/carbon composites is the carbonization of carbon fibre reinforced plastics (CFRP). In this process, the shrinkage of the matrix is hindered by the fibres and leads to a high amount of cracks resulting in a microscopic open porosity. To control this process, it is necessary to gain knowledge about its essential parameters, in which the crack microstructure plays an important role. Micrographs (SEM) revealed that the cracks can be distinguished in three different types: fibre-matrix debonding, segmentation cracks and micro-delaminations. Fibre-matrix bonding determines which crack type dominates the structure of the final carbon/carbon composite. The evolution of the cracks during pyrolysis (temperature, sequence and importance of the crack types) was investigated by means of acoustic emission and microscopy in combination with a heating stage. By comparing these results with those of thermogravimetric analysis and dilatometer experiments, the development of the cracks can be explained.

KEYWORDS: carbon/carbon composites, CFRP, carbonization, microstructure, crack evolution, heating stage, acoustic emission

INTRODUCTION

The carbonization of carbon fibre reinforced plastics (CFRP) is the major process for manufacturing carbon/carbon composites (C/C). In addition the carbonization can be used with different fibres or precursors to produce a variety of ceramic matrix composites (CMC). All these materials have a common characteristic: the hindered shrinkage of the matrix due to the fibres leads to a high amount of matrix cracking. This requires further densification steps to reach good mechanical properties. It is normally achieved by reinfiltrating the porous intermediate state with the same or a similar precursor as used in the primary step. The DLR-Institute of Structures and Design uses liquid silicon instead to infiltrate the C/C, which reacts with most of the carbon matrix to silicon carbide [1].

In order to control the carbonization process, it is necessary to gain knowledge about its essential parameters, in which the crack microstructure plays an important role. Basic research work was conducted to understand the development of this structure during carbonization.

RESULTS

Investigations were conducted with a CFRP (fibre volume fraction: 60 %), which consists of woven Tenax™ HTA-fibres (a PAN-derived standard type fibre; plain weave, 3000 filaments per roving) and a totally aromatic, nitrogen containing, thermosetting precursor. A variation in fibre-matrix bonding can be achieved by thermally pretreating the fibres which leads to a reduction of the functional groups on the surface. In this case a material with non-pretreated laminates was used. The CFRP was manufactured by resin transfer moulding (RTM), cured at 200 °C and post-cured for eight hours at 240 °C.
Thermogravimetric analysis of CFRP (figure 1) shows, that the carbonization can be distinguished in four major stages [2]. The post-curing stage occurs at temperatures approaching 420 °C. It is based on further polyaddition reactions. Up to approximately 650 °C the main pyrolysis takes place with high mass losses of 10 %. During the next stage the mass losses occur at a slower rate. Gradual dehydrogenation takes place, and from 1000 °C onwards nitrogen is evolved. The last stage beyond 1200 °C is dominated by healing reactions. Thermogravimetry of the HTA-fibre revealed, that reactions start in the fibre at 900 °C (not shown). This is the main reason for further mass losses in the annealing stage.

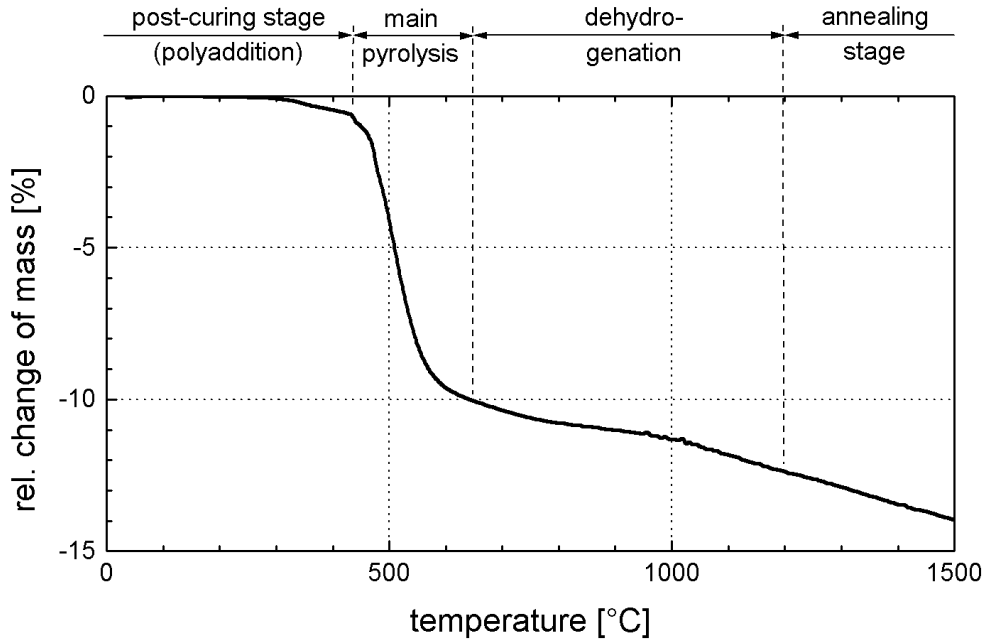

Fig. 1: The four stages of carbonization of the tested CFRP

The results from the dilatometry of the resin and the CFRP (perpendicular to the laminate plane) are presented in figure 2. In this figure, the changes of the CFRP (solid line) and the resin (dashed line) are shown. A calculated curve (dotted line) is added, which represents the results of the resin multiplied with the matrix volume fraction, so that this curve can be compared with the CFRP one to find out the characteristics of the reinforcement.
During the post-curing stage both materials show thermal expansion, which for the case of the resin has a maximum at the glass transition temperature (T_g = 310 °C). At the onset of pyrolysis, accelerating shrinkage can be observed in the case of the resin, while the CFRP reveals a

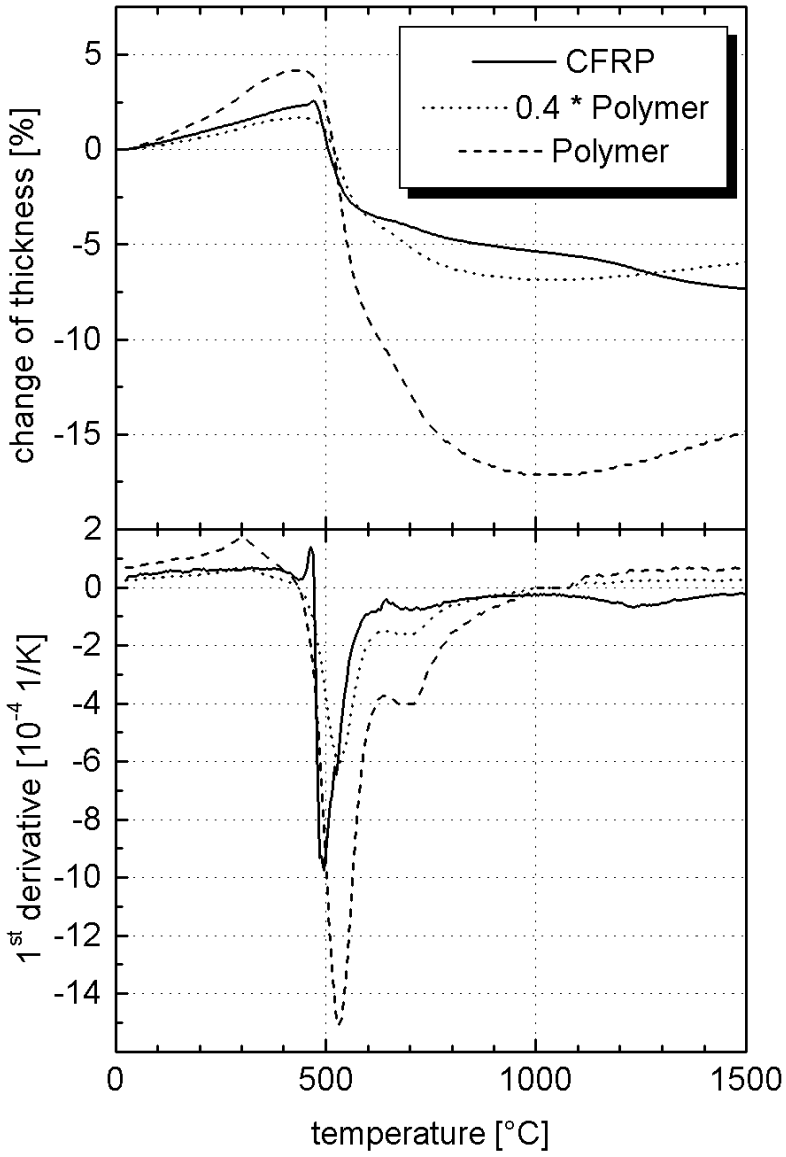

Fig. 2: Dilatometer experiments of resin and CFRP

slight shrinkage, followed by a distinct maximum of expansion. Beyond 460 °C, the CFRP starts shrinking heavily, too. During the main pyrolysis, the CFRP loses 6.5 % in thickness, whereas the resin loses 15 %. In this stage three temperatures are important: At about 505 °C both specimens reach their former length. The maximum shrinkage occurs at 540 °C. Beyond 575 °C the CFRP curve and the calculated curve of the resin show clearly different characteristics: CFRP seems to have an effect which can partly compensate the shrinkage of the resin. During the dehydrogenation stage, the resin shows a second maximum in shrinkage. In the annealing stage, the resin exhibits again thermal expansion, while the CFRP shrinks due to the assumed reactions within the fibre. The total shrinkage in thickness is 7.5 % (CFRP) and 15 % (resin) at 1500 °C.

Micrographs (SEM, figure 3), taken after thermal treatment, indicate, that the cracks can be distinguished in three different types: on the mesoscale segmentation cracks (a), which divide the fibre bundles in segments, micro-delaminations in the boundaries mainly between warp and weft threads (b) and fibre-matrix debonding (c) on the microscale. Due to the hindered shrinkage parallel (but not perpendicular) to the reinforcement plane, the segmentation cracks have a high degree of orientation.

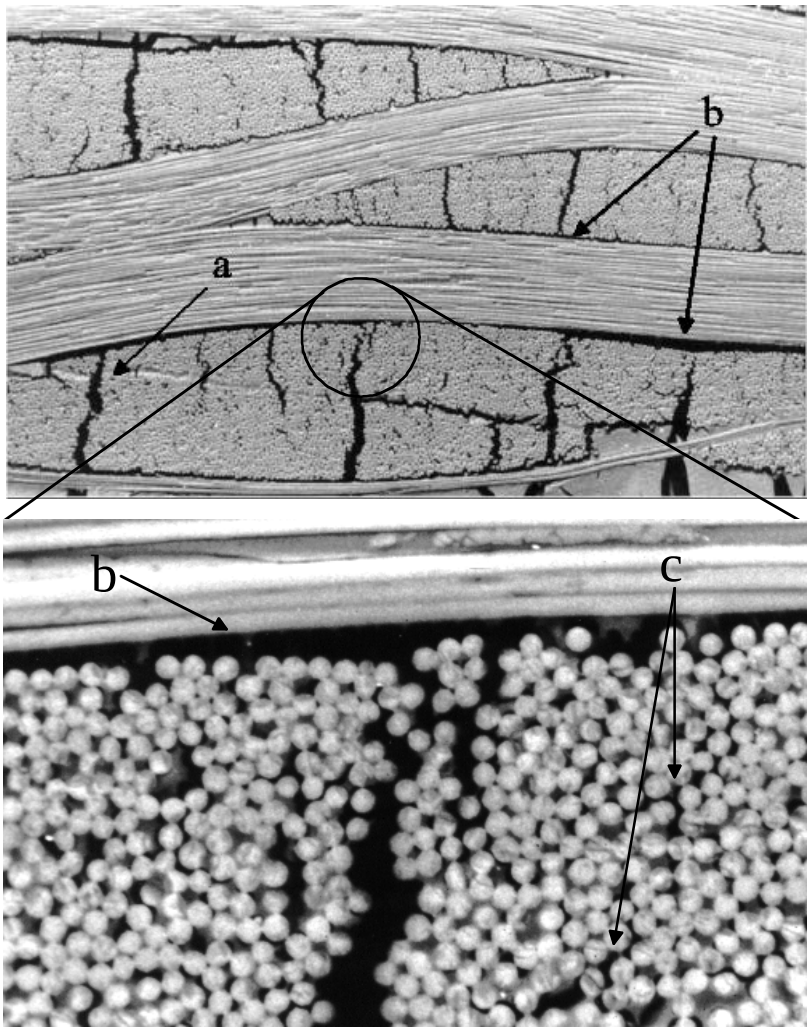

Fig. 3: Segmentation cracks (a), micro- delaminations (b) and fibre- matrix- delaminations (c) after carbonization of CFRP at approximately 900 °C

The evolution of these types of cracks during pyrolysis was investigated by means of acoustic emission and thermo-optical analysis (TOA). Both procedures make in situ investigations possible. The thermo-optical analysis means a microscope equipped with a heating stage, which permits a direct observation of thermal processes. However, only surfaces can be studied and cracks must reach a certain dimension to become visible. In these items lie the advantages of the acoustic emission analysis. Acoustic emission is an effect referring to the bulk material. Cracks emit events which are simultaneously measured, so that the temperature ranges of the development of the crack types can be determined.

The results of the acoustic emission analysis are presented in figure 4. There the heating phase of the carbonization of a CFRP sample with a maximum temperature of 700 °C is shown. Significant acoustic emission can be detected in two temperature ranges. The first one endures from 400 °C to 475 °C. Further emission cannot be observed until 510 °C, where it starts at first with low energies, but beyond 550 °C the specimen emits high amounts of acoustic signals.

Micrographs taken during a thermal treatment up to 890 °C from the thermo-optical analysis are presented in figure 5. The three pictures on the left hand side were taken with an enlargement of 500x. These show a large resin area with two fibre bundles crossing the picture plane and another one running in the plane. The three micrographs on the right hand side each show three fibre bundles crossing the picture plane and three running in the plane (from two only the edges can be seen).

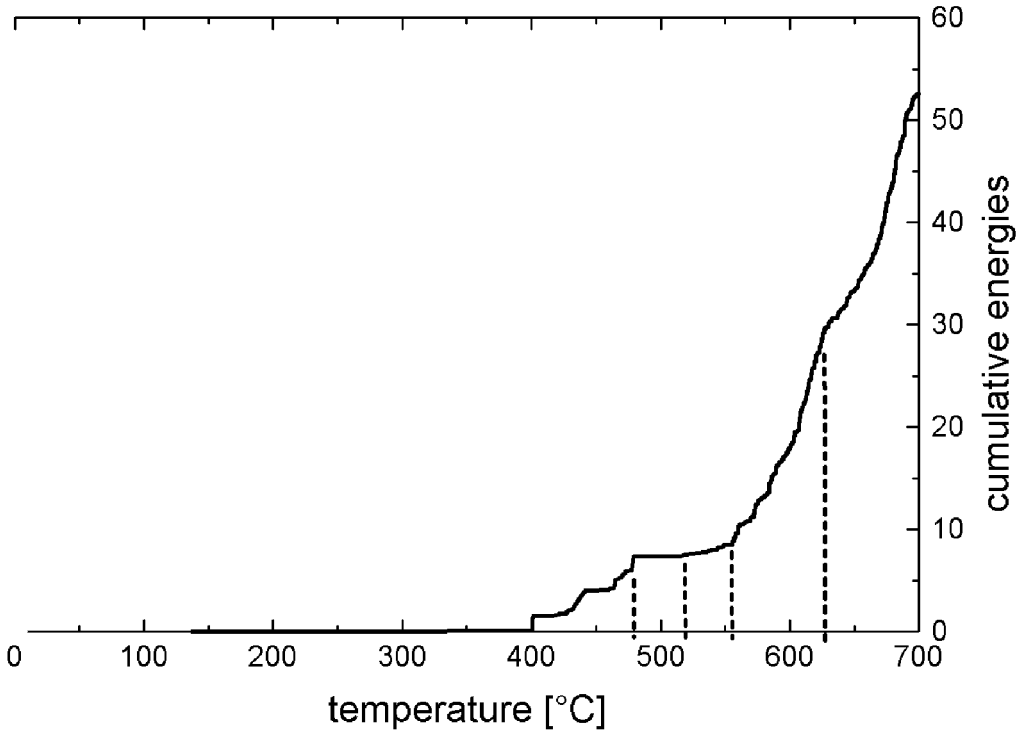

Fig. 4: Acoustic emission during pyrolysis of the used CFRP (heating phase)

At the start of the experiment (top, left) low fibre-matrix-debonding can be observed, especially at the rim of the fibre bundles. This is caused by the post-curing at 240 °C. Up to 510 °C (middle, left) this condition does not change appreciably. Fibre-matrix-debonding becomes more distinct, but in the inner parts of the bundles debonding occurs only occasionally, normally at close-spaced filaments. In the following temperature range this condition changes rapidly. Up to 545 °C (bottom, left) debonding occurs clearly in the bundle, too. The observation in this temperature range becomes more and more difficult because of a surface effect: due to the heavy shrinkage of the resin the matrix recedes out of the focus plane. But the filaments are at least partly imbedded in the resin. This results in a curved surface, so that the light is not reflected back into the microscope. This effect causes dark rims at the filaments, so that it becomes difficult to recognize the debonded filaments. In the micrograph on the upper right hand side, the specimen is shown at 550 °C with an enlargement of 200x. It seems that the fibre-matrix-delaminations at the rim of the fibre bundles have yet interconnected to micro-delaminations. Up to 600 °C (middle, right) the segmentation cracks have evolved. Comparing to the maximum temperature of 890 °C (bottom, right) the main crack pattern seems to be completed at about 620 °C. The cracks become clearly broader, but only few cracks are added, which are irregularly oriented (in contrast to the segmentation cracks and micro-delaminations).

DISCUSSION

In interpreting the effects of the pyrolysis the highly anisotropic behaviour of the carbon fibre must be taken into account. The HTA-fibre has a CTE parallel to the longitudinal axis, which rises continuously from $-0.1 \cdot 10^{-6}$ 1/K (room temperature) to $3 \cdot 10^{-6}$ 1/K (1000 °C) [3]. Perpendicular to the fibre axis of standard type PAN-fibres values of $10\text{-}18 \cdot 10^{-6}$ 1/K (room tempera-

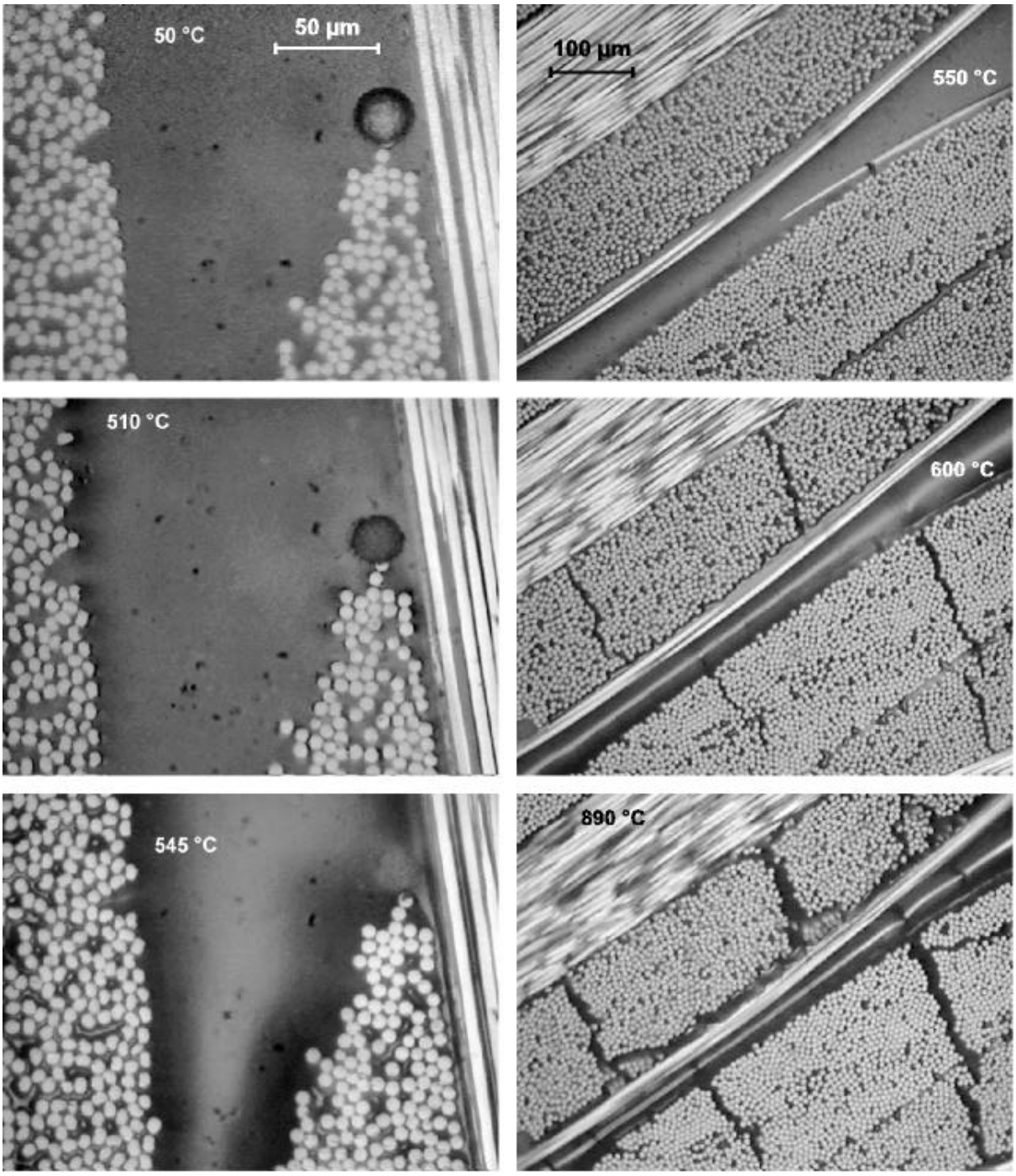

Fig. 5: Thermo-optical analysis of the pyrolysis of the used CFRP

ture) [4,5] and $13 \cdot 10^{-6}$ 1/K (20 °C - 1300 °C)[1] [6] can be found. The polymer matrix material has a CTE of $50 \cdot 10^{-6}$ 1/K (after post-curing). This results in a distinct thermal mismatch in the laminates.

It can be assumed, that the temperature of the (nearly) stress-free state of the CFRP is the temperature of post-curing. Thus, when this temperature is passed at the beginning of the carbonization, the fibre bundles (filaments plus matrix) are submitted to compression perpendicular and tension parallel to the fibre axis due to the thermal mismatch (Fig.6, top). In the stage of post-curing further reactions take place, as it was shown by the thermogravimetrical analysis. In addition the polymer precursor reveals a viscoelastic behaviour (loss factor $\tan\delta \approx 0.13$

[1] This value was measured with the Celanese G50-fibre, which corresponds closely to the HTA-fibre.

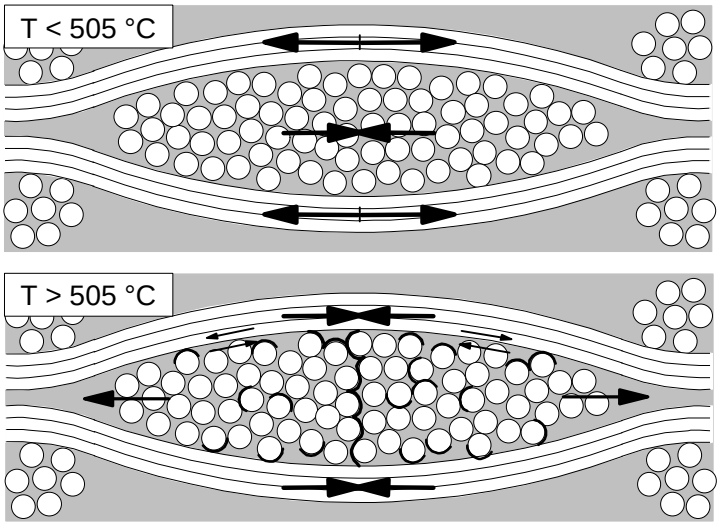

Fig.6: Stress distribution in CFRP during pyrolysis

at T_g = 310 °C, measured with DMA). This results in stress relaxation. When the material is cooled down, before the onset of pyrolysis is reached, segmentation cracks and micro-delaminations in the polymer matrix may be generated [7].

With the onset of pyrolysis at 420 °C, high amounts of reaction gases are generated in the matrix which are trapped at first in the still compact material. These gases diffuse in neighbouring pores, where they cause high pore pressures. The pores start to expand and interconnect until the thus generated network reaches the surface and the gases can leave the material [8]. This is the explanation for the acoustic emission in the first temperature range from 400 °C to 475 °C. This effect can be studied by dilatometry, too. Due to the fibre reinforcement, the pressures must be high for the extension of the pores. This results in a short term expansion of the CFRP in thickness [9], which has been measured in the dilatometer experiment in the temperature range from 420 °C to 460 °C. In the case of the relative brittle neat polymer specimen, only small pressures are necessary to generate the network, so that this effect cannot be observed there.

It is clear that in this temperature range matrix and fibres are still stressed in compression perpendicular to the fibre axis. This changes at about 500 °C. Dilatometer experiments revealed that at about 505 °C the both specimens reached their original length. Considering stress relaxation, which takes place when the post-curing temperature is passed, it can be assumed, that the stress state must change before this temperature is exceeded. Therefore tensile stress in matrix and fibres is quickly developing perpendicular and compressive stress parallel to the fibre axis (Fig.6, bottom).

The micrographs from the thermo-optical analysis indicated that at temperatures above 510 °C fibre-matrix-debonding and above 550 °C the segmentation cracks evolved. The material is under high residual stress due to the heterogeneous composition. It is clear that at first the stress peaks exceed the critical stress for crack initiation, which causes debonding and a homogenization of the stress curve. This is accompanied by a slight rise in the cumulative energy curve of the acoustic emission analysis. When the averaged stress passes the critical stress (for crack initation), the segmentation cracks evolve from single debondings by connecting all fissures which are on the crack path. Their high degree of orientation results from the fact that the composite can shrink in thickness, but not in plane. The onset of their evolution is marked by the kink in the cumulative energy curve (≈550 °C).

According to the thermo-optical analysis it seems, that the micro-delaminations have evolved at 550 °C. This would mean, that the transmission of the forces beyond the interfaces between warp and weft fibres would not be possible, so that the segmentation cracks could not develop. In this context it must be considered that with microscopes, only surfaces can be observed. But

on the surface additional stresses can occur (e.g. free-edge-delaminations), which do not exist in the bulk. It can be concluded that the development of the micro-delaminations is not complete until higher temperature. The dilatometer experiments may solve this problem. At 575 °C the curve of the CFRP clearly flattens in contrast to the one of the resin. This may be caused by the micro-delaminations, which lead to expansion and can thus partly compensate the shrinkage of the matrix. When the micro-delaminations emerge, the force can no longer be transmitted, so that the cracks, which evolve at higher temperatures, are caused by local stresses in the segments and are thus irregularly oriented.

CONCLUSIONS

A general characterization of the carbonization of CFRP was conducted by means of thermogravimetry and dilatometry. The development of the crack pattern was then investigated in situ with acoustic emission and thermo-optical analysis. SEM-micrographs revealed, that the cracks can be divided in three types: fibre-matrix-debonding, segmentation cracks and micro-delaminations. The micrographs obtained on the heating stage demonstrate, that the evolution of the main crack pattern takes place in the temperature range 500 °C to roughly 620 °C. In the first step, the fibre-matrix-debonding develops, because stress peaks exceed the critical stress for crack initiation. Beyond 550 °C, the segmentation cracks evolve since the averaged stress of the fibre bundle exceeds the critical value for crack propagation. The segmentation cracks start from single debondings and connect all fissures that are on the crack path. Micro-delaminations seem to emerge at 575 °C. With the origin of micro-delaminations the development of the main crack pattern is complete; further cracking occurs due to local stresses in the inner parts of the segments. Finally it can be established, that both thermo-optical and acoustic emission analysis present a suitable approach to the investigation of the pyrolysis of CFRPs.

ACKNOWLEDGEMENTS

The authors would like to express their gratitude especially to the German Research Community (DFG) for backing this project as part of the Graduiertenkolleg 285 („Interfaces in Crystalline Materials“). Furthermore we would like to thank Mr. K. Luthardt, Leica Microsystems GmbH, Wetzlar, Germany for supporting the experiments with the heating stage, and all colleagues from the DLR-Institute of Structures and Design for the valuable help and discussion.

REFERENCES

[1] Krenkel, W., Gern, F.: Microstructure and Characteristics of CMC Manufactured via the Liquid Phase Route, *Proceedings of the Ninth International Conference on Composite Materials*, Madrid, Spain, July 12-16, 1993, Vol. II: Ceramic Matrix Composites and Other Systems, pp. 173-181.

[2] Jenkins, G.M., Kawamura, K.: *Polymeric Carbons- Carbon Fibre, Glass and Char*, Cambridge University Press, London, 1976.

[3] Hillermeier, Tenax Ltd.: dilatometer measurements

[4] Savage, G.: *Carbon-Carbon Composites*, Chapman & Hall, London, 1993, p. 54.

[5] Wulfhorst, B., Becker, G.: Faserstoff-Tabellen: Carbonfasern, *Chemiefasern/ Textilindustrie*, Vol. 39/91, No. 12, 1989, Deutscher Fachbuchverlag, Frankfurt/Main.

[6] Sheaffer, P.M.: Transverse Thermal Expansion of Carbon Fibers, *Extended Abstracts of the eighteenth Biennial Conference on Carbon*, American Chemical Society, 1987, pp. 20-21.
[7] Schulte-Fischedick, J., Frieß, M., Krenkel, W., König, M.: Untersuchung der Entstehung des Rißmusters während der Pyrolyse von CFK-Vorkörpern zur Herstellung von C/C-Werkstoffen, *Tagungsband der Werkstoffwoche ´98*, Munich, 12.-15.10.1998 (in print).
[8] Nam, J.-D., Seferis, J.C.: Initial polymer degradation as a process in the manufacture of carbon-carbon composites, *Carbon*, Vol. 30, No. 5, 1992, pp. 751-761.
[9] Wang, C.J.: The effect of resin thermal degradation on thermostructural response of carbon-phenolic composites and the manufacturing process of carbon-carbon composites, *Journal of Reinforced Plastics and Composites*, Vol. 15, No. 10, 1996, pp. 1011-1026.